

# First-principles study on methane storage properties of porous graphene modified with Mn

**Yingjie Zhao**

Lanzhou University of Technology

**Yuhong Chen** (✉ [lzchenyh@163.com](mailto:lzchenyh@163.com))

Lanzhou University of Technology <https://orcid.org/0000-0003-1597-1232>

**Wenhui Xu**

Lanzhou University of Technology

**Meiling Zhang**

Lanzhou University of Technology

**Cuicui Sang**

Lanzhou University of Technology

**Cairong Zhang**

Lanzhou University of Technology

---

## Research Article

**Keywords:** Porous graphene, Mn modified, Methane, First principles

**Posted Date:** May 5th, 2021

**DOI:** <https://doi.org/10.21203/rs.3.rs-449932/v1>

**License:**   This work is licensed under a Creative Commons Attribution 4.0 International License.

[Read Full License](#)

---

**Version of Record:** A version of this preprint was published at Applied Physics A on November 19th, 2021.  
See the published version at <https://doi.org/10.1007/s00339-021-05084-6>.

# First-principles study on methane storage properties of porous graphene modified with Mn

Yingjie Zhao<sup>1</sup>, Yuhong Chen<sup>1,2\*</sup>, Wenhui Xu<sup>1</sup>, Meiling Zhang<sup>1</sup>, Cuicui Sang<sup>1</sup>, Cairong Zhang<sup>1,2</sup>

<sup>1</sup> School of Science, Lanzhou University of Technology, Lanzhou 730050, China

<sup>2</sup> State Key Laboratory of Advanced Processing and Recycling of Non-Ferrous Metals, Lanzhou, University of Technology, Lanzhou 730050, China

\* Correspondence: lzchenyh@163.com; Tel.: +86-931-297-3780

## Abstract:

Porous graphene (PG) has a promising future in gas storage due to its unique pore characteristics and large specific surface area. The adsorption properties of PG and PG modified by Mn atoms (Mn-PG) for CH<sub>4</sub> molecules have been studied based on first-principles density functional theory. It was found that the optimal adsorption position of CH<sub>4</sub> on PG was the carbon annulus pore, and the adsorption energy was -0.174 eV. The optimal position of the PG system modified by a single Mn atom is the central hole of the carbon ring, and the optimal position of the two Mn atoms is that Mn atoms are respectively located at different carbon ring holes on the opposite side of PG, with an average binding energy of -4.101 eV. The modification of Mn atom enhances the electronegativity of PG substrate and forms a negative charge center at the carbon ring, which is beneficial to enhance the adsorption performance of CH<sub>4</sub> molecules with positive charge on the surface. The CH<sub>4</sub> molecules are adsorbed on the PG surface through the electrostatic interaction with Mn atoms and PG substrates as well as the intermolecular force of CH<sub>4</sub> molecules. Mn-PG system can adsorb 6 CH<sub>4</sub> molecules on one side, and the average adsorption energy is -0.345 eV. When PG was modified with two Mn atoms, 12 CH<sub>4</sub> molecules could be adsorbed on both sides, and the average adsorption energy was -0.338 eV, the adsorption capacity can reach 38.43 wt.%.

**Keywords:** Porous graphene; Mn modified; Methane; First principles

## 1. Introduction

With the development of science and technology, people have been exploring the earth deeply, but at the same time, it also brings various problems such as energy depletion and environmental pollution. The combustion of coal, oil and other fossil fuels will produce CO<sub>2</sub> and a large number of harmful gases [1]. The main component of natural gas is methane (CH<sub>4</sub>) [2]. Compared with other fossil fuels, CH<sub>4</sub> combustion produces less CO<sub>2</sub>, and the energy produced by a CH<sub>4</sub> is 3.1 times that of H<sub>2</sub>. Natural gas is rich in resources all over the world, and it is an important transition fuel to achieve low-carbon energy [3]. In addition, methane is a greenhouse gas, escaping into the atmosphere will aggravate the greenhouse effect, accounting for about 20% of global warming [4]. The adsorption and storage of methane gas is a hot topic in scientific research, which is an effective means to solve the greenhouse effect and low-carbon energy substitution problem. Therefore, it is necessary to seek a kind of efficient, safe and large reserves of methane storage materials. Methane storage materials are mostly characterized by porous structure. Zeolite [5], molecular sieves [6], activated carbon [7], covalent organic framework materials (COFs) [8], metal organic framework materials (MOFs) [9, 10] are common gas storage materials. Menon et al. [11] pointed out that the storage capacity of CH<sub>4</sub> has an obvious linear relationship with the surface area of molecular sieve and other materials. The larger the surface area, the more adsorption capacity, but the upper limit is lower. Jackson et al. [12] found that a high-porosity boron-nitride polymer had a CH<sub>4</sub> adsorption capacity of 18.1 cm<sup>3</sup>/g at 273 K, and also had a good adsorption effect on H<sub>2</sub> and CO<sub>2</sub>. Rozyyev et al. [13] showed that methane storage of porous polymer COP-150 reached 62.5 wt.% under 5~100bar cyclic pressure, and it had a certain memory effect. Liang et al. [14] pointed out that a porous metal-organic framework ST-2 can store the same amount of methane at 130 bar and 298 K as the CNG storage method at 250 bar, and the maximum storage capacity can reach 289 cm<sup>3</sup>/cm<sup>3</sup> under high pressure. Chen et al. [15] found that the metal cluster super porous metal organic skeleton materials (NU-1501-M, M=Al or Fe) met the four standards of BET at the same time. The methane storage performance was excellent,

among which the storage capacity of NU-1501-Al type material for high pressure methane was 66.0 wt.%. Liu et al. [16] found that the adsorption capacity of CH<sub>4</sub> in DUT-49 MOF materials can reach 24.0 wt.%, and pointed out that the surface area, pore size and pore volume of MOFs and COFs have an important influence on the gas storage capacity of CH<sub>4</sub>. According to the standard proposed by the Advanced Research Projects Agency-Energy (ARPA-E) of the U.S. Department of energy (DOE), the weight density of CH<sub>4</sub> adsorption by vehicle energy should be greater than 50.0 wt.% [17]. Although some materials have reached this standard, they are stored under high pressure or high temperature, so it is difficult to apply them in practice.

Graphene is a two-dimensional material, and its unique nanostructure gives it excellent thermal conductivity [18], mechanical [19], optical [20] and electrical [21] properties. It is a strong competitor in the fields of sensors, composites and energy storage [22], as well as a potential medium for methane storage. Yang et al. [23] pointed out that the adsorption energy of CH<sub>4</sub> on graphene increased with the increase of graphene layers, and the maximum is -0.267 eV, indicating that the adsorption of CH<sub>4</sub> on intrinsic graphene is weak. The adsorption performance of gas can be improved by regulating the electronic structure of graphene through defects, doping or metal element modification [24-26]. Ghanbari et al. [27] simulated the adsorption of CH<sub>4</sub> on Ag-modified graphene using Quantum-Espresso software, and calculated that the adsorption energy of CH<sub>4</sub> could reach -0.399 eV in aerobic environment, which was much higher than the adsorption energy on the intrinsic graphene. Rad et al. [28] found that CH<sub>4</sub> has higher adsorption energy, more charge transfer, smaller adsorption distance and stronger interaction on Pt modified graphene than intrinsic graphene through Gaussian software, and the adsorption energy of CH<sub>4</sub> can reach -0.485 eV. However, due to the small pore defects of the graphene structure itself and the limited adsorption space, the overall adsorption capacity is low.

Porous graphene is a two-dimensional structure derived from graphene. There are nano pores with adjustable size and shape on the structure, and it has the porous structure common to energy storage materials. It has been found that porous graphene with different geometrical configurations will exhibit different properties of

semiconductor, semi-metal or metal [29]. The existence of defects makes it have larger specific surface area and more active sites compared with intrinsic graphene, which creates good conditions for gas adsorption and storage [30-32]. Bieri et al. [33] successfully prepared a porous graphene (PG) composed of two  $C_6H_3$  rings through experiments, with pore spacing of 7.400 Å. The mass of the porous graphene in the same size crystal cell is about two-thirds that of the intrinsic graphene, and it has a larger specific surface area, showing good gas adsorption performance. Chen et al. [34] used Material Studio software to calculate that the double-sided porous graphene modified with Sc atoms could adsorb 12  $H_2$  molecules with a hydrogen storage capacity of 9.09 wt.%. Yuan et al. [35] found that 14  $H_2$  molecules could be adsorbed on the porous graphene structure by using Y atoms modified double-sided, with an average adsorption energy of -0.230 eV and a hydrogen storage capacity of 7.87 wt.%. Previous studies [36] found that Mn atom modification can significantly improve the adsorption performance of graphene for  $CH_4$ . When two Mn atoms were modified, the system could adsorb 10  $CH_4$  molecules, with an average adsorption energy of -0.402 eV and an adsorption capacity of 32.93 wt. %, but there was still a large gap with the storage target of DOE in the US. In order to improve the adsorption capacity of  $CH_4$ , based on PG structure, Mn atom was used to modify porous graphene, and its adsorption performance was studied. It is expected to provide theoretical support for the research and development of safe and efficient methane storage.

## 2. Calculation Methods and Models

The calculation used in this study employs the CASTEP module under Material Studio 8.0 software [37], based on the first-principles pseudopotential plane wave method considering density functional theory. A generalized gradient approximation (GGA) [38] under the Perdew–Burke–Ernzerhof (PBE) exchange correlation functional form is chosen, and the super soft pseudopotential is used to describe the interaction between electrons and ions. Because the adsorption of  $CH_4$  molecules on the PG surface is weak, and the GGA functional may underestimate the weak adsorption energy, the Van der Waals correction (i.e., DFT-D method) is used in the calculation [39]. All

the atoms in the calculation were completely relaxed, and the convergence criterion of structure optimization was that the force of each atom was less than 0.03 eV/Å, the energy difference was less than  $1.0 \times 10^{-6}$  eV/atom, and the self-consistent field convergence threshold was  $1.0 \times 10^{-6}$  eV/atom. By testing the cut-off energy and K-point sampling of the system, considering the calculation accuracy and calculation cost, the cut-off energy is selected as 400 eV, and the K-point sampling in the Brillouin zone is  $5 \times 5 \times 1$ . The calculation of the porous graphene crystal cell satisfies the periodic boundary conditions, and the vacuum layer is 25 Å to avoid interlayer interaction.

The binding energy ( $E_b$ ) and average binding energy ( $\bar{E}_b$ ) of the Mn atom on PG are defined as:

$$E_b = E_{n\text{Mn+PG}} - E_{(n-1)\text{Mn+PG}} - E_{\text{Mn}} \quad (1)$$

$$\bar{E}_b = (E_{n\text{Mn+PG}} - E_{\text{PG}} - nE_{\text{Mn}})/n \quad (2)$$

Where  $E_{n\text{Mn+PG}}$  and  $E_{(n-1)\text{Mn+PG}}$  respectively represent the total energy of PG modified by  $n$  and  $(n-1)$  Mn atoms (Mn-PG),  $E_{\text{PG}}$  is the total energy of PG, and  $E_{\text{Mn}}$  is the energy of a free Mn atom.

The adsorption energy ( $E_{\text{ad}}$ ) and average adsorption energy ( $\bar{E}_{\text{ad}}$ ) of the CH<sub>4</sub> molecule are defined as

$$E_{\text{ad}} = E_{i\text{CH}_4+n\text{Mn+PG}} - E_{(i-1)\text{CH}_4+n\text{Mn+PG}} - E_{\text{CH}_4} \quad (3)$$

$$\bar{E}_{\text{ad}} = (E_{i\text{CH}_4+n\text{Mn+PG}} - E_{n\text{Mn+PG}} - iE_{\text{CH}_4})/i \quad (4)$$

Where  $E_{i\text{CH}_4+n\text{Mn+PG}}$  and  $E_{(i-1)\text{CH}_4+n\text{Mn+PG}}$  respectively represent the total energy of  $n\text{Mn-PG}$  system with  $i$  and  $i-1$  CH<sub>4</sub> molecules, and  $E_{\text{CH}_4}$  is the energy of a free CH<sub>4</sub> molecule.

In the Mn modified PG structure, the calculation formula of stored methane mass density (CH<sub>4</sub> molecule adsorption capacity) is defined as:

$$\text{CH}_4(\text{wt. \%}) = \left[ \frac{m_{\text{CH}_4}}{m_{\text{CH}_4} + m_{n\text{Mn+PG}}} \right] \times 100 \quad (5)$$

Where  $m_{\text{CH}_4}$  and  $m_{n\text{Mn+PG}}$  respectively represent the mass of CH<sub>4</sub> molecules and PG system modified by  $n$  Mn atoms.

The optimized geometry of PG protocell is shown in Fig.1(a), and the lattice constant is 7.480 Å, which is in good agreement with the experimental value of 7.400

Å [33]. The structure is composed of two C<sub>6</sub>H<sub>3</sub> rings, or it can be regarded as the formation of H atom saturated dangling bond after removing part of C atom in 3×3 graphene supercell. The direct band gap of porous graphene was calculated to be 2.398 eV, which was basically consistent with the 2.400 eV calculated by Rao et al. [40] through VASP software, indicating that the calculation model used in this paper is correct, the calculation method and calculation accuracy are reasonable, and the calculation results are reliable.

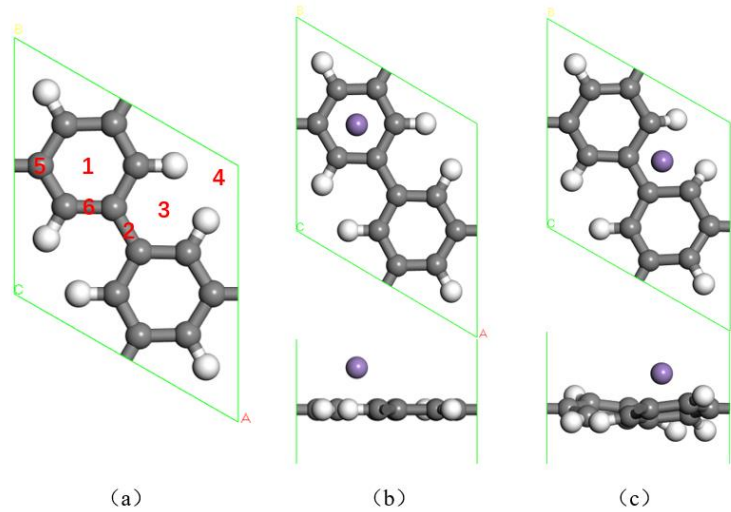


**Fig. 1** (a) The geometric structure of PG unit cell; (b)~(c) Two stable geometric structures of PG system modified by Mn atom (gray, white and purple spheres represent C, H and Mn atoms respectively)

### 3. Results and Discussion

#### 3.1 Adsorption performance of CH<sub>4</sub> molecules on porous graphene

In the porous graphene system, six symmetric adsorption sites as shown in Fig. 1 (a) are considered: 1 is the carbon ring hole, 5 is the C top of the carbon ring, 6 is the C-C bridge in the carbon ring, 2 is the bridge between the two carbon rings, 3 is the carbon-hydrogen ring hole, and 4 is the center of the carbon-hydrogen macrocycle. After placing CH<sub>4</sub> molecules in the above six initial positions for geometric structure optimization, the optimal adsorption position of CH<sub>4</sub> molecules on the porous graphene system was explored by calculating the adsorption energy. It is found that the best adsorption position of single CH<sub>4</sub> molecule on the porous graphene system is the top position of position 1, as shown in Fig. 2, where the adsorption energy is -0.174 eV, and

the distance between CH<sub>4</sub> molecule and PG substrate is 3.353 Å. This is similar to the optimal adsorption position of CH<sub>4</sub> in the intrinsic graphene structure, which is the central hole of carbon ring. It can be seen that the adsorption energy of CH<sub>4</sub> molecule in PG system is lower, but it has more adsorption sites than that in intrinsic graphene system. Therefore, based on the research of Mn atom modified intrinsic graphene, we continue to use Mn atom modified porous graphene system, hoping to further improve the adsorption performance of PG system for CH<sub>4</sub> molecule and improve the adsorption energy of CH<sub>4</sub> molecule.

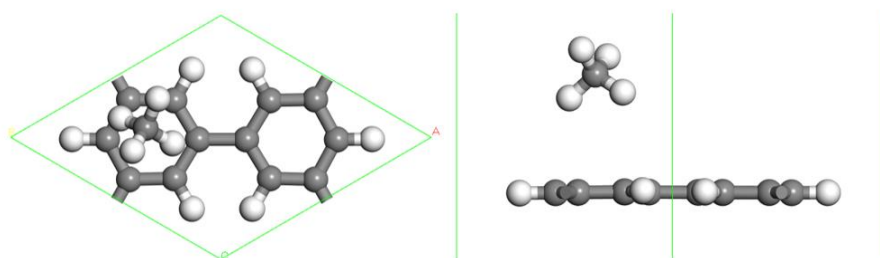


**Fig. 2** Geometric structure of the optimal adsorption position of a single CH<sub>4</sub> molecule on PG system.

## 3.2 Geometric structure of PG system modified by Mn atom

### 3.2.1 Geometric structure of PG modified by single Mn atom

Firstly, the optimal modification position of a single Mn atom on the PG system was studied, and the six initial positions as shown in Fig.1 (a) were also selected for optimization test. The results show that the Mn atoms at position 5 and 6 relax to position 1 after optimization, and the Mn atoms at position 2 relax to position 3 after optimization. The Mn atoms at position 4 cannot be adsorbed on the PG system, while the Mn atoms at position 1 and 3 can be adsorbed stably. It can be seen that the PG system modified by a single Mn atom has two stable structures, as shown in Fig.1 (b)~(c), respectively. The binding energies of Mn atom are -4.017 eV and -3.134 eV, respectively. In Fig. 1 (b), the binding energy of Mn atom is the largest and the substrate structure is more stable, which is the optimal modification position of Mn atom in PG system (that is, the central hole of carbon ring). The distance between Mn atom and PG substrate is 1.503 Å.

From Table.1, the Mulliken charge population of PG system before and after Mn modification (C1~C6 are the six C atoms in the carbon ring where Mn atom is located

on the PG substrate), it can be seen that after Mn atom is adsorbed on PG system, the Mn atom loses 1.11 e, the positive charge increases, the PG substrate gains electrons, the negative charge increases, and the carbon ring surrounded by C1~C6 gets more electrons, forming an obvious negative charge center. An electric field is generated between the two, which causes a small part of electrons on C atom in the PG system to transfer to the lower energy orbital of Mn atom, resulting in Dewar [41] effect. The interaction between Mn and PG can also be seen from the partial state of the density (PDOS) of Mn PG system shown in Fig. 3 (a). In the range of -2.20~-0.34 eV, the 2p orbital of C atom and the 3d orbital of Mn atom overlap strongly. In the range of 0~0.72 eV, the s, p and d orbitals of Mn atom overlap with the 2p orbital of C atom, indicating that there is a strong orbital hybridization between Mn and PG. This action makes the Mn atoms adsorb stably on the PG surface.

**Table.1** The Mulliken charge population of CH<sub>4</sub> molecule, PG system and Mn-PG system adsorbed for the 1-6 CH<sub>4</sub> molecules. (charge/e)

	H1	H2	H3	H4	C	C1	C2	C3	C4	C5	C6	Mn
<b>CH<sub>4</sub></b>	0.27	0.27	0.28	0.27	-1.10	-	-	-	-	-	-	-
<b>PG</b>	-	-	-	-	-	-0.01	-0.22	-0.01	-0.22	-0.01	-0.22	-
<b>Mn-PG</b>	-	-	-	-	-	-0.13	-0.37	-0.13	-0.37	-0.13	-0.37	1.11
<b>1st CH<sub>4</sub></b>	0.24	0.28	0.08	0.06	-1.05	-0.13	-0.37	-0.15	-0.37	-0.13	-0.37	1.56
<b>2nd CH<sub>4</sub></b>	0.27	0.24	0.07	0.11	-1.02	-0.14	-0.37	-0.14	-0.37	-0.14	-0.37	1.92
<b>3rd CH<sub>4</sub></b>	0.24	0.25	0.22	0.25	-1.00	-0.14	-0.37	-0.14	-0.37	-0.14	-0.37	1.95
<b>4th CH<sub>4</sub></b>	0.25	0.25	0.23	0.20	-0.98	-0.14	-0.37	-0.14	-0.38	-0.14	-0.37	1.99
<b>5th CH<sub>4</sub></b>	0.25	0.27	0.27	0.22	-1.03	-0.14	-0.37	-0.15	-0.37	-0.15	-0.36	2.00
<b>6th CH<sub>4</sub></b>	0.22	0.21	0.22	0.21	-0.94	-0.15	-0.38	-0.15	-0.39	-0.15	-0.38	2.04

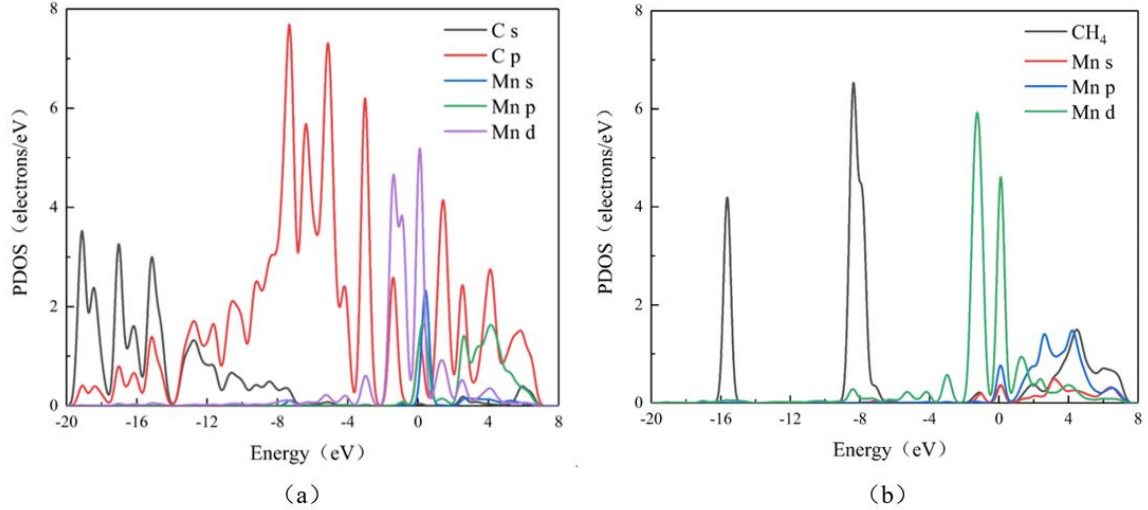


**Fig. 3** PDOS of the system (a) Mn PG; (b) Mn PG adsorbs a CH<sub>4</sub>

### 3.2.2 Geometric structure of PG modified by two Mn atoms

There are three stable structures after the optimization of the PG structure modified by two Mn atoms, as shown in Fig. 4 (a) ~ (c). In Fig. 4 (a), two Mn atoms are located in the center of two carbon rings on the same side; in Fig. 4 (b), the two Mn atoms are located on both sides of the same carbon ring center, and are symmetrical with respect to PG surface; in Fig. 4 (c), two Mn atoms are located in the center of different carbon rings on different sides respectively, showing a centrally symmetric structure relative to the PG substrate. In the structure shown in Fig. 4 (b), the average binding energy of Mn atom is -3.119eV, and the substrate is partially deformed and the overall stability of the structure is poor. In Fig. 4 (a) and Fig. 4 (c), the average binding energy of Mn atom is -4.176 eV and -4.101 eV, respectively. The substrate has no obvious deformation, and the average binding energy value of Mn atom is greater than its cohesion energy -2.920eV [42], so the possibility of Mn atom agglomeration is avoided. It can be seen that when two Mn atoms modify PG system, they can be adsorbed on the same or different sides of different carbon rings.

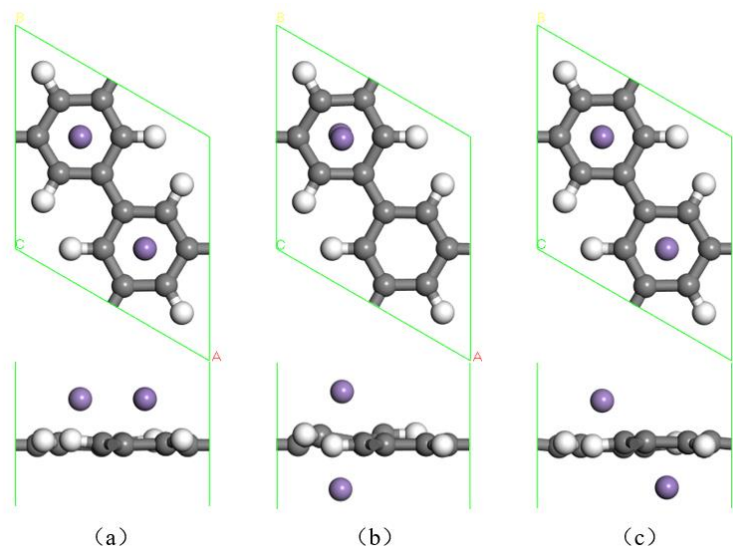


**Fig. 4** Three stable geometric structures of PG system modified by two Mn atoms.

### 3.3 Adsorption performance of CH<sub>4</sub> on Mn modified PG system

#### 3.3.1 Adsorption of CH<sub>4</sub> on Mn-PG system

The most stable structure of the single Mn atom modified PG system is shown in Fig. 1 (b). CH<sub>4</sub> has several adsorption positions on Mn PG system, including Mn atom top, C-C bridge position, hydrocarbon ring hole position and C-atom top position. Studies have found that the most stable adsorption site of CH<sub>4</sub> molecules is above Mn atom near the C-H bond, as shown in Fig. 5 (a). At this point, the adsorption energy of CH<sub>4</sub> molecule is -0.840 eV, which is much higher than that of CH<sub>4</sub> molecule on unmodified porous graphene (-0.174 eV). This indicates that Mn atom modification greatly improves the adsorption performance of PG for CH<sub>4</sub> molecule and enhances the adsorption energy of CH<sub>4</sub> molecule on PG. In order to study the interaction mechanism, Fig. 3 (b) shows the partial density of states of Mn-PG system when adsorbing a CH<sub>4</sub> molecule. It can be seen from the figure that there is no orbital coupling phenomenon between the 3d orbital of Mn atom and the orbital of CH<sub>4</sub> molecule, so there is a weak interaction between the two. The adsorption of CH<sub>4</sub> molecule on PG belongs to physical adsorption.

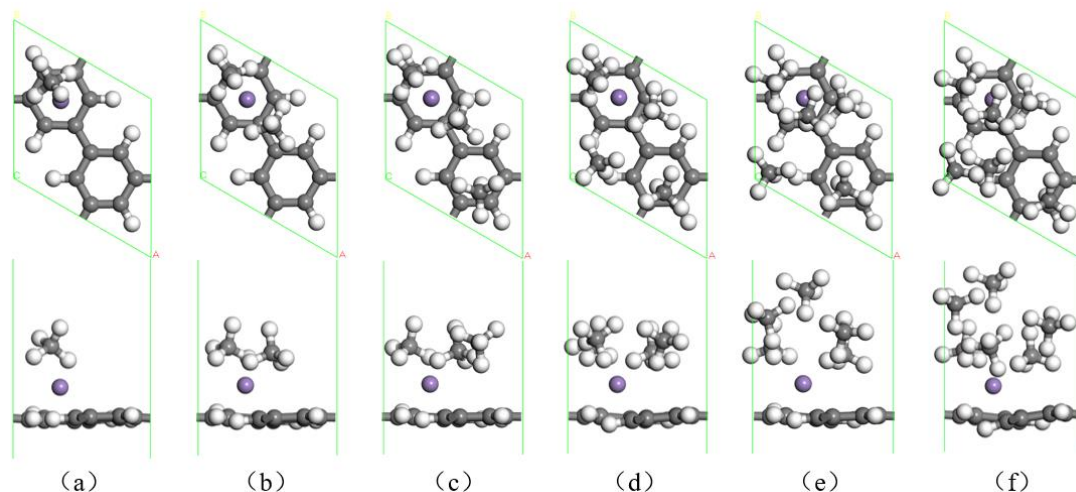


**Fig. 5** Geometric structure of Mn-PG system adsorbed 1-6 CH<sub>4</sub> molecules.

In order to study the adsorption capacity of CH<sub>4</sub> in Mn-PG system, the adsorption conditions of multiple CH<sub>4</sub> molecules on Mn-PG system were further calculated. It was found that up to 6 CH<sub>4</sub> molecules could be adsorbed on one side, and the optimized structure was shown in Fig. 5 (a) ~ (f). It can be seen that CH<sub>4</sub> molecules are mainly adsorbed around Mn atoms or above the carbon ring. When the fifth CH<sub>4</sub> molecule is adsorbed, the adsorption space of CH<sub>4</sub> molecules in the same plane tends to be saturated and stratification occurs. Table.2 lists the adsorption energy ( $E_{ad}$ ), and average adsorption energies ( $\bar{E}_{ad}$ ) of the CH<sub>4</sub> molecule on the PG system, the distance  $d_{Mn-PG}$  between the Mn atom and the PG plane, the distance  $d_{Mn-CH_4}$  between the C atom and the Mn atom in each CH<sub>4</sub> molecule of the Mn-PG system, and the distance  $d_{PG-CH_4}$  between the CH<sub>4</sub> molecule and PG plane when Mn-PG system adsorption 1-6 CH<sub>4</sub> molecules. It can be seen that the distance between Mn atom and PG plane is basically unchanged during the continuous adsorption of CH<sub>4</sub> molecules, which indicates that the two-dimensional structure of Mn-PG system remains stable and does not deform or collapse with the increase of the number of CH<sub>4</sub> molecules adsorbed.

Table.1 also lists the Mulliken charge population of CH<sub>4</sub> molecule, Mn-PG system and Mn-PG system adsorb 1-6 CH<sub>4</sub> molecules, in which C and H1-H4 are carbon atoms and four hydrogen atoms on CH<sub>4</sub> molecule respectively. It can be seen that after the first CH<sub>4</sub> molecule adsorption, Mn atoms lose 0.45 e, and a small amount of electrons (0.07 e) transfer to PG substrate further enhance the negative electrical properties of the

substrate. Most electrons (0.38 e) transfer to CH<sub>4</sub> molecules, H3 and H4 atoms near Mn atom get electrons 0.20 e and 0.21 e respectively. H2 and C atoms lose a small amount of electrons, and the molecules show polarity. After the adsorption of the second CH<sub>4</sub> molecule, Mn atom further loses electrons (0.36 e), and H atom in CH<sub>4</sub> molecule gains electrons. H3 and H4 close to Mn atom get 0.21 e and 0.16 e, respectively. The second CH<sub>4</sub> molecule also shows strong polarity. After adsorption, CH<sub>4</sub> molecules are negatively charged as a whole and interact with positively charged Mn atoms, which enhances the adsorption performance of CH<sub>4</sub> molecules. As the number of CH<sub>4</sub> molecules increases, the adsorption energy of CH<sub>4</sub> molecules decreases. When the 3rd ~ 6th CH<sub>4</sub> molecules are adsorbed, the distance between CH<sub>4</sub> molecules and Mn atoms is longer, the charge transfer is less, and the electrostatic interaction is weak. However, the modification of Mn atom enhances the overall electronegativity of PG substrate and forms the negative charge center. It makes the surface of CH<sub>4</sub> molecule with positive electricity on the PG surface far away from the modified atom the adsorption can also be produced, which is mainly caused by the interaction between the positive charge on the surface of CH<sub>4</sub> and the substrate with negative charge. The adsorption energy of the fifth CH<sub>4</sub> molecule is much lower than that of the other CH<sub>4</sub> molecules, which is due to the stratification phenomenon when the fifth CH<sub>4</sub> molecule is adsorbed, which makes the CH<sub>4</sub> molecule far away from the PG substrate and weakens the interaction. The sixth CH<sub>4</sub> molecule is closer to the PG surface than the fifth CH<sub>4</sub> molecule, which is located in the first layer of CH<sub>4</sub> molecule adsorption. The addition of the sixth CH<sub>4</sub> molecule makes the position of most of the original CH<sub>4</sub> molecules relax, so the adsorption energy is increased compared with the fifth CH<sub>4</sub> molecule. The Mn-PG system adsorbed six CH<sub>4</sub> molecules on one side, one more CH<sub>4</sub> molecule than the Mn modified intrinsic graphene system, and the atoms number of porous graphene was less than that of intrinsic graphene, so the adsorption capacity of CH<sub>4</sub> molecule was improved.

**Table.2** Energy parameters and geometric parameters of CH<sub>4</sub> molecule adsorption on Mn-PG system.

Number of CH <sub>4</sub>	1	2	3	4	5	6
$E_{ad}$ (eV)	-0.840	-0.665	-0.231	-0.133	-0.074	-0.125
$\bar{E}_{ad}$ (eV)	-0.840	-0.753	-0.579	-0.467	-0.389	-0.345
$d_{Mn-PG}$ (Å)	1.528	1.558	1.554	1.557	1.550	1.605
$d_{Mn-CH_4}$ (Å)	2.169	2.327	5.357	3.881	4.354	3.678
$d_{PG-CH_4}$ (Å)	3.429	3.190	3.661	3.551	5.834	3.497

Fig. 6 shows the charge differential density diagram of Mn-PG system adsorbing 1~3 CH<sub>4</sub> molecules. The blue and yellow isosurface represent the electron gain and electron loss regions respectively. It can be seen that there are more charge transfer between the first and second CH<sub>4</sub> molecules and Mn atoms, CH<sub>4</sub> molecules show obvious polarity after adsorption, and CH<sub>4</sub> molecules have strong interaction, so the adsorption energy is larger, and the number of CH<sub>4</sub> molecules is promoted. The charge transfer of the third to sixth CH<sub>4</sub> molecules is less, which is not obvious in the same precision charge difference diagram, which is the same as the result of Mulliken charge population analysis; The polarity and intermolecular interaction of CH<sub>4</sub> molecules are weak after adsorption. They are mainly due to the electrostatic interaction between the positive charge on the surface of CH<sub>4</sub> molecule and the negatively charged PG substrate.

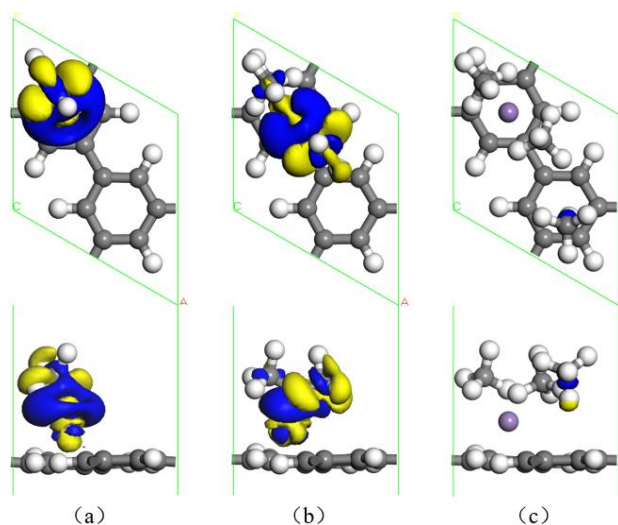


**Fig. 6** Charge difference density diagram of Mn-PG system adsorbed 1~3 CH<sub>4</sub> molecules.

### 3.3.2 Adsorption of CH<sub>4</sub> on PG system modified by two Mn atoms

When the PG system is modified by two Mn atoms, the energies of the two stable structures shown in Fig. 4 (a) and Fig. 4 (c) are almost the same. After the adsorption test of CH<sub>4</sub> molecule, it is found that the substrate of the structure in Fig. 4 (a) will undergo obvious bending deformation after the CH<sub>4</sub> molecule is adsorbed. This is due to the electrostatic interaction between the two Mn atoms and CH<sub>4</sub> molecule on the same side of the PG surface, and the difference between the Mn atom itself and its carbon ring the strong force makes the PG substrate bend to the surface of CH<sub>4</sub> molecule, which destroys its two-dimensional structure. The structure in Fig. 4 (c) remains a stable two-dimensional structure after the adsorption of CH<sub>4</sub>. Therefore, the structure in Fig. 4 (c) is selected to study the adsorption performance of CH<sub>4</sub> molecules in the PG system modified by two Mn atoms. In the two Mn atom modified PG system, 12 CH<sub>4</sub> molecules can be adsorbed on both sides, and 6 CH<sub>4</sub> molecules can be adsorbed on each side. The optimized geometric structures are shown in Fig. 7 (a) ~ (l). It can be seen that the distance between the two Mn atoms and PG remains unchanged during the continuous adsorption of CH<sub>4</sub>, and the two-dimensional structure of the substrate is stable. The adsorption position of CH<sub>4</sub> molecule is basically the same as that of single Mn atom. Each side of CH<sub>4</sub> molecule is first adsorbed near Mn atom, and Mn atom plays an important role in the adsorption process of CH<sub>4</sub> molecule. The first four CH<sub>4</sub> molecules are adsorbed on one side in the same plane. When the fifth CH<sub>4</sub> molecule is adsorbed, due to the repulsive force between CH<sub>4</sub> molecules, a large number of CH<sub>4</sub> molecules can't coexist in the same plane, so stratification occurs. At the same time, CH<sub>4</sub> molecules in the first layer relax, and the adsorption space reaches saturation after adsorption of six CH<sub>4</sub> molecules. When CH<sub>4</sub> molecules adsorbed on both sides of the system are saturated, the overall structure is more symmetrical. Fig. 8 shows the continuous adsorption energy  $E_{ad}$ , the average adsorption energy  $\bar{E}_{ad}$  of CH<sub>4</sub> molecules in the two Mn atom modified PG system, and the distance  $d_{PG-CH_4}$  from the CH<sub>4</sub> molecule to the PG plane. It can be seen that the distance between the CH<sub>4</sub> molecules in the first layer on each side and the PG surface is 0.3~0.4 Å, and the adsorption energy decreases with the increase of the number of CH<sub>4</sub> molecules adsorption, ranging from -0.853 eV to -0.114 eV. The distance between the CH<sub>4</sub>

molecules in the second layer and the PG surface is more than  $0.5\text{\AA}$ , and the adsorption energy is generally lower than  $-0.100\text{eV}$ . This is because the distance between the  $\text{CH}_4$  molecules in the second layer and the PG surface is far, and the interaction between the positively charged  $\text{CH}_4$  molecules on the surface and the negatively charged PG substrate is weak and the adsorption energy is low. When 12  $\text{CH}_4$  molecules were adsorbed, the average adsorption energy was  $-0.338\text{ eV}$ , and the adsorption capacity was up to  $38.43\text{ wt.}\%$ . Compared with Mn modified intrinsic graphene [36], the average adsorption energy changed little, but the adsorption capacity increased by  $5.50\text{ wt.}\%$ , which further approached the energy storage target proposed by DOE of the United States.

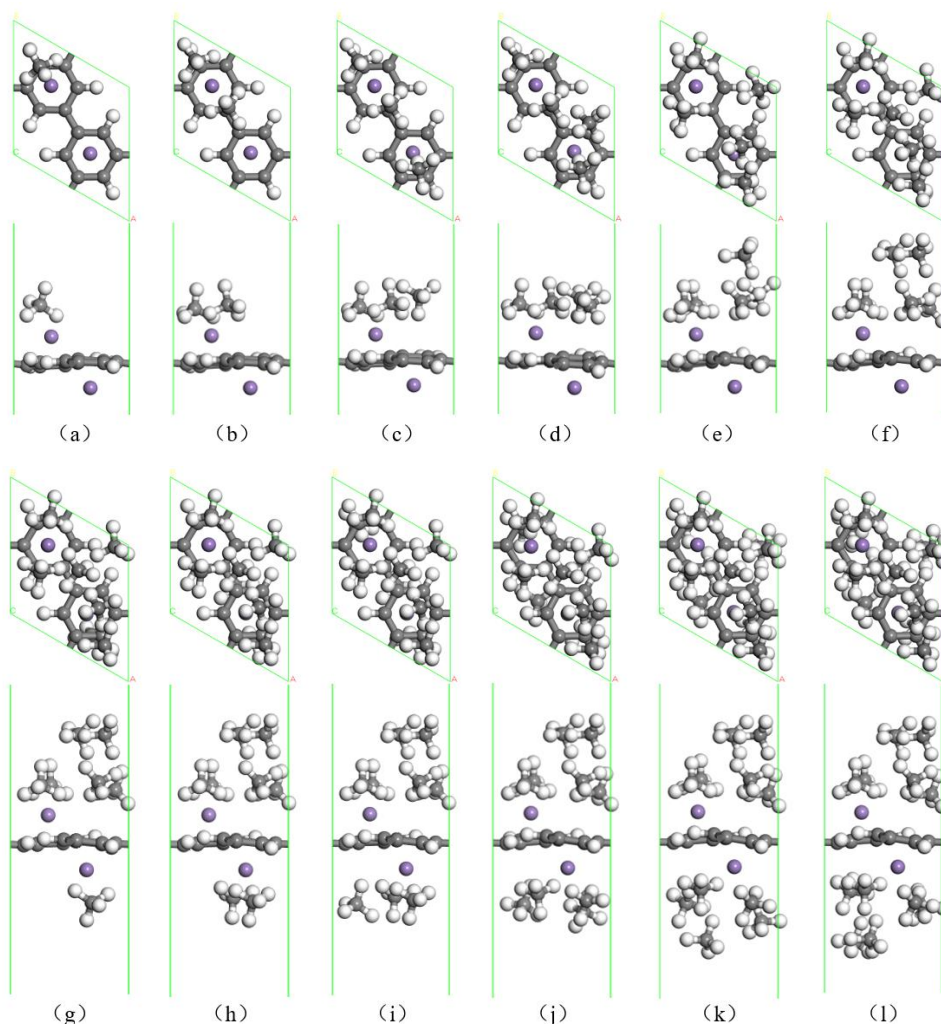


**Fig. 7** Geometric structure of two Mn atoms modified PG system adsorbed 1~12  $\text{CH}_4$  molecules.

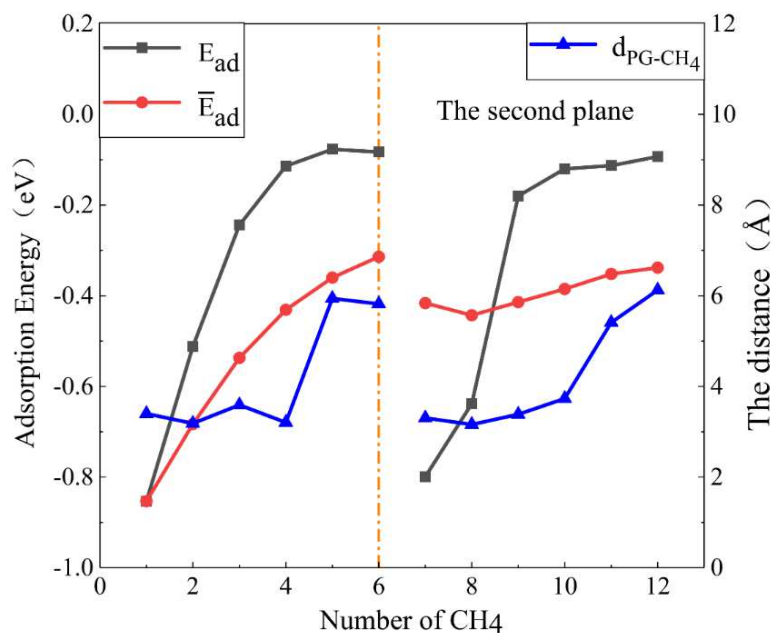


**Fig. 8** Energy parameters and geometric parameters of two Mn atoms modified PG system adsorbed 1~12 CH<sub>4</sub> molecules.

In order to further verify the structural stability and eliminate the influence of edge effect, a super large cell was established based on the above porous graphene structure, which contains 96 C atoms, 216 H atoms and 8 modified Mn atoms. This structure can adsorb 48 CH<sub>4</sub> molecules, and the optimized geometry is shown in Fig. 9. The results show that the average binding energy of Mn atom is -4.045 eV, which is larger than the cohesive energy and avoids the agglomeration. The average adsorption energy of CH<sub>4</sub> molecule is -0.292 eV, which is less different from the calculation results of protocell. It shows that the system structure is stable and the calculation results are reasonable. There is no CH<sub>4</sub> molecule adsorption at the intermediate pore of the supercrystalline cell, which is due to the large pore size of the PG structure. The CH<sub>4</sub> molecule located here is far away from the negative charge center of the substrate and Mn atom, and the interaction force is too weak for adsorption to occur. It can be seen that the pore size has a great influence on the adsorption performance of CH<sub>4</sub> molecules. We will conduct subsequent studies on the adsorption performance of CH<sub>4</sub> by adjusting the pore size of PG system.

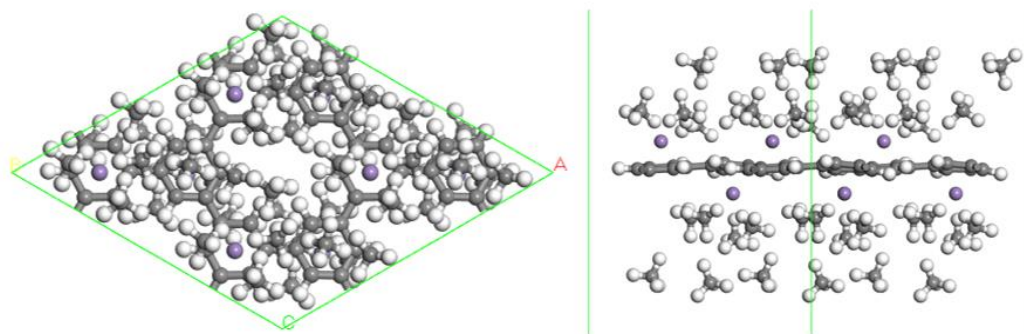


**Fig. 9** Geometric structure of Mn-PG supercell system adsorbed CH<sub>4</sub> molecules.

#### 4. Conclusion

Based on first-principles density functional theory, the adsorption properties of PG and Mn-PG systems for CH<sub>4</sub> molecules were studied, and the following conclusions were drawn:

(1) The optimum adsorption location of CH<sub>4</sub> molecule on porous graphene is the carbon annulus pore, with the adsorption energy of -0.174 eV and the distance between CH<sub>4</sub> molecule and PG substrate is 3.353 Å.

(2) The optimal position of the PG system modified by a single Mn atom is the central hole of the carbon ring. When two Mn atoms modified PG system, only the system with two Mn atoms located at different carbon annulus sites on the opposite side can maintain the structural stability, and the average binding energy is -4.101 eV. The charge transfer between Mn atom and PG substrate resulted in strong orbital hybridization, which made it stably modified on PG surface. The modification of Mn atom enhances the electronegativity of PG substrate and generates a negative charge center at the carbon ring, which is beneficial to enhance the adsorption performance of CH<sub>4</sub> molecules with positive charge on the surface.

(3) Mn atom modification can improve the adsorption performance of CH<sub>4</sub> molecules in the porous graphene system. The best adsorption position of a single CH<sub>4</sub> molecule in the Mn-PG system is above Mn atom near the C-H bond, and the adsorption energy can reach -0.840 eV, which belongs to physical adsorption. The CH<sub>4</sub> molecules are adsorbed on the PG surface through the electrostatic interaction with Mn atoms and PG substrates as well as the synergistic effect of the intermolecular forces of CH<sub>4</sub>. The

CH<sub>4</sub> molecules close to Mn atoms are negatively charged on the whole, and have strong electrostatic interactions with positively charged Mn atoms, resulting in large adsorption energy. Moreover, the polarity of the molecules reduces the intermolecular repulsion, which is conducive to the increase of the number of CH<sub>4</sub> molecules adsorption. The positively charged CH<sub>4</sub> molecules on the surface far from Mn atoms have weak electrostatic interactions with the negatively charged PG substrate and negatively charged center, resulting in low adsorption energy.

(4) Mn-PG system can adsorb 6 CH<sub>4</sub> molecules on one side, and the average adsorption energy is -0.345 eV. When PG is modified by two Mn atoms, 12 CH<sub>4</sub> molecules can be adsorbed on both sides with an average adsorption energy of -0.338 eV and an adsorption capacity of 38.43 wt.%, which is close to the energy storage target proposed by DOE of the United States. Therefore, PG is a kind of methane storage material with good development prospect.

## **Acknowledgements**

The authors gratefully acknowledge the financial support from the National Natural Science Foundation of China [grant number 51562022]; the Basic Scientific Research Foundation for Gansu Universities of China [grant number 05-0342], and the Special Program for Applied Research on Super Computation of the NSFC-Guangdong Joint Fund (second phase).

## **Authors' contributions**

Y. Zhao, Y. Chen, W. Xu, M. Zhang, C. Sang, and C. Zhang all contributed to the writing of this manuscript, and all authors have given their approval to the final version.

**Data availability** All the data and materials are available.

## **Compliance with ethical standards**

**Conflict of interest** The authors declare that they have no conflict of interest.

**Ethics approval** All authors agree with ethical responsibilities of authors.

**Consent to participate** All authors consent to participate.

**Consent for publication** All authors consent for publication.

## Reference:

- [1] Jacobson MZ (2005). *J Geophys Res-Atmos* 110:D14105
- [2] Keppler F,Hamilton JTG,Brass M,Rockmann T (2006). *Nature* 439:187-191
- [3] Makal TA,Li JR,Lu W,Zhou HC (2012). *Chem Soc Rev* 41:7761-7779
- [4] Feldman DR,Collins WD,Biraud SC,Risser MD,Turner DD,Gero PJ,Tadić J,Helmig D,Xie S,Mlawer EJ,Shippert TR,Torn MS (2018). *Nat Geosci* 11:238-243
- [5] Fraenkel D,Shabtai J (1977). *J Am Chem Soc* 99:7074-7076
- [6] Chen S,Dai W,Luo J,Tang Y,Wang C,Sun W (2009). *Acta Phys-Chim Sin* 25:285-290
- [7] Policicchio A,Maccallini E,Agostino RG,Ciuchi F,Aloise A,Giordano G (2013). *Fuel* 104:813-821
- [8] Furukawa H,Yaghi OM (2009). *J Am Chem Soc* 131:8875-8883
- [9] Ma S,Zhou H (2010). *Chem Commun* 46:44-53
- [10] Wu H,Simmons JM,Liu Y,Brown CM,Wang XS,Ma S,Peterson VK,Southon PD,Kepert CJ,Zhou HC,Yildirim T,Zhou W (2010). *Chemistry* 16:5205-5214
- [11] Menon VC,Komarneni S (1998). *J Porous Mat* 5:43-58
- [12] Jackson KT,Rabbani MG,Reich TE,El-Kaderi HM (2011). *Polym Chem-UK* 2:2775-2777
- [13] Rozyyev V,Thirion D,Ullah R,Lee J,Jung M,Oh H,Atilhan M,Yavuz CT (2019). *Nat Energy* 4:604-611
- [14] Liang C,Shi Z,He C,Tan J,Zhou HD,Zhou HL,Lee Y,Zhang YB (2017). *J Am Chem Soc* 139:13300-13303
- [15] Chen Z,Li P,Anderson R,Wang X,Zhang X,Robison L,Redfern LR,Moribe S,Islamoglu T,Gomez-Gualdrón DA,Yildirim T,Stoddart JF,Farha OK (2020). *Science* 368:297-303
- [16] Liu J,Zou R,Zhao Y (2016). *Tetrahedron Lett* 57:4873-4881
- [17] The Advanced Research Projects Agency–Energy DE-FOA-0000672: Methane Opportunities for Vehicular Energy (MOVE).(2012) DOE Available from: [https://arpa-e-foa.energy.gov/Default.aspx?Search=move&SearchType=.](https://arpa-e-foa.energy.gov/Default.aspx?Search=move&SearchType=)

- [18] Balandin AA, Ghosh S, Bao W, Calizo I, Teweldebrhan D, Miao F, Lau CN (2008). Nano Lett 8:902-907
- [19] Lee C, Wei X, Kysar JW, Hone J (2008). Science 321:385-388
- [20] Nair RR, Blake P, Grigorenko AN, Novoselov KS, Booth TJ, Stauber T, Peres NM, Geim AK (2008). Science 320:1308
- [21] Heersche HB, Jarillo-Herrero P, Oostinga JB, Vandersypen LM, Morpurgo AF (2007). Nature 446:56-59
- [22] Novoselov KS, Geim AK, Morozov SV, Jiang D, Zhang Y, Dubonos SV, Grigorieva IV, Firsov AA (2004). Science 306:666-669
- [23] Yang D, Yang N, Ni J, Xiao J, Jiang J, Liang Q, Ren T, Chen X (2017). Mater Design 119:397-405
- [24] Ganji MD, Mazaheri H, Khosravi A (2015). Commun Theor Phys 64:576-582
- [25] Gautam M, Jayatissa AH (2012). Solid State Electron 78:159-165
- [26] Zhou M, Lu Y, Cai Y, Zhang C, Feng Y (2011). Nanotechnology 22:385502
- [27] Ghanbari R, Safaiee R, Golshan MM (2018). Appl Surf Sci 457:303-314
- [28] Rad AS, Pazoki H, Mohseni S, Zareyee D, Peyravi M (2016). Mater Chem Phys 182:32-38
- [29] Jiang L, Fan Z (2014). Nanoscale 6:1922-1945
- [30] Du A, Zhu Z, Smith SC (2010). J Am Chem Soc 132:2876-2877
- [31] Carr LD, Lusk MT (2010). Nat Nanotechnol 5:316-317
- [32] Ao Z, Dou S, Xu Z, Jiang QG, Wang GX (2014). Int J Hydrogen Energy 39:16244-16251
- [33] Bieri M, Treier M, Cai J, Ait-Mansour K, Ruffieux P, Groning O, Groning P, Kastler M, Rieger R, Feng X, Mullen K, Fasel R (2009). Chem Commun 45:6919-6921
- [34] Chen Y, Wang J, Yuan L, Zhang M, Zhang C (2017). Materials 10:894
- [35] Yuan L, Chen Y, Kang L, Zhang C, Wang D, Wang C, Zhang M, Wu X (2017). Appl Surf Sci 399:463-468
- [36] Zhao Y, Chen Y, Song M, Liu X, Xu W, Zhang M, Zhang C (2020). Adv Theor Simul 3:2000035
- [37] Segall MD, Lindan PJD, Probert MJ, Pickard CJ, Hasnip PJ, Clark SJ, Payne MC

- (2002). *J Phys-Condens Mat* 14:2717-2744
- [38] Perdew JP, Burke K, Ernzerhof M (1996). *Phys Rev Lett* 77:3865-3868
- [39] Bjorkman T, Gulans A, Krasheninnikov AV, Nieminen RM (2012). *Phys Rev Lett* 108:235502
- [40] Rao D, Lu R, Meng Z, Wang Y, Lu Z, Liu Y, Chen X, Kan E, Xiao C, Deng K, Wu H (2014). *Int J Hydrogen Energy* 39:18966-18975
- [41] Mingos DMP (2001). *J Organomet Chem* 635:1-8
- [42] Kittel C, Hellwarth RW (1957). *Phys Today* 10:43-44

# Figures

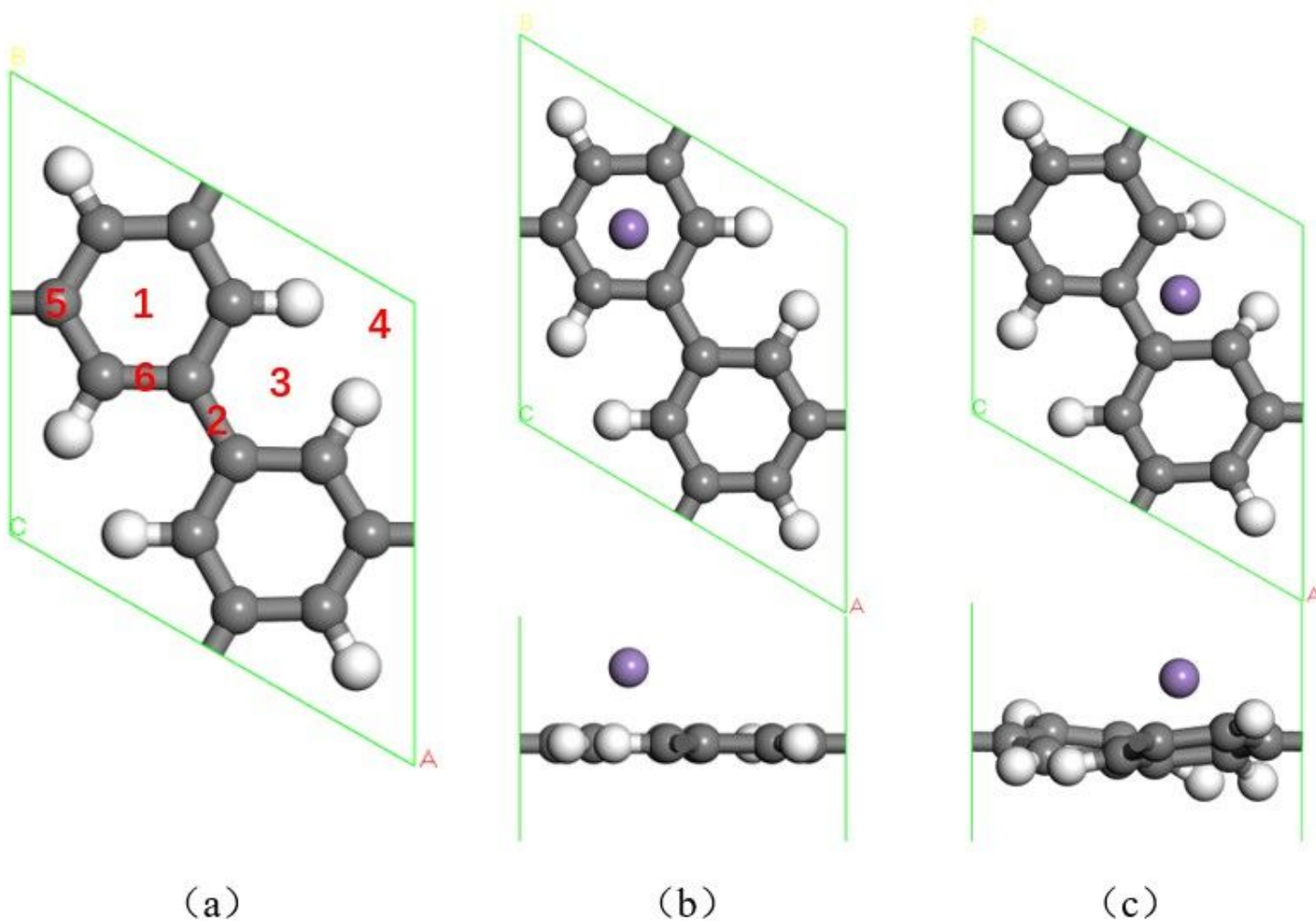


Figure 1

(a) The geometric structure of PG unit cell; (b)~(c) Two stable geometric structures of PG system modified by Mn atom (gray, white and purple spheres represent C, H and Mn atoms respectively)

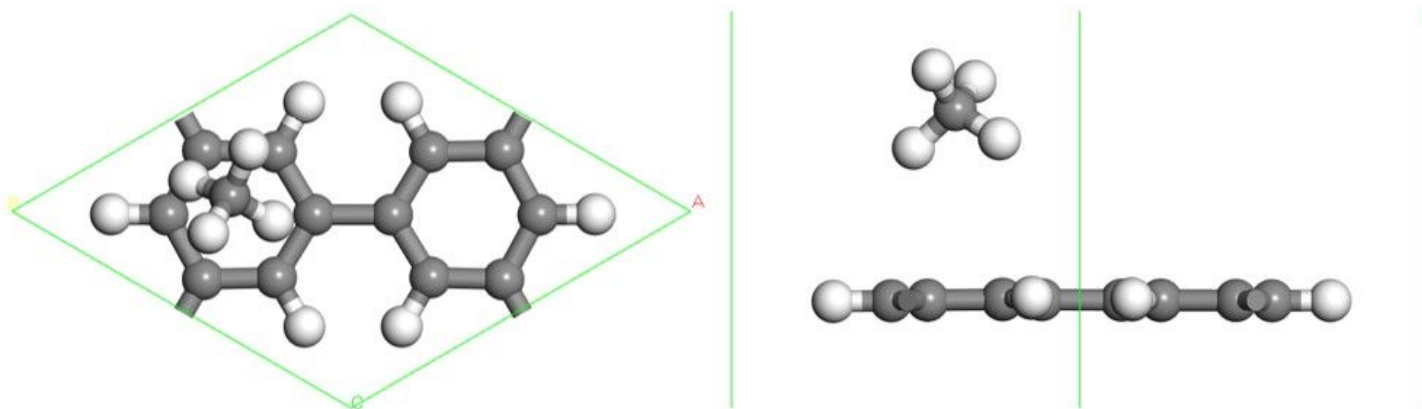
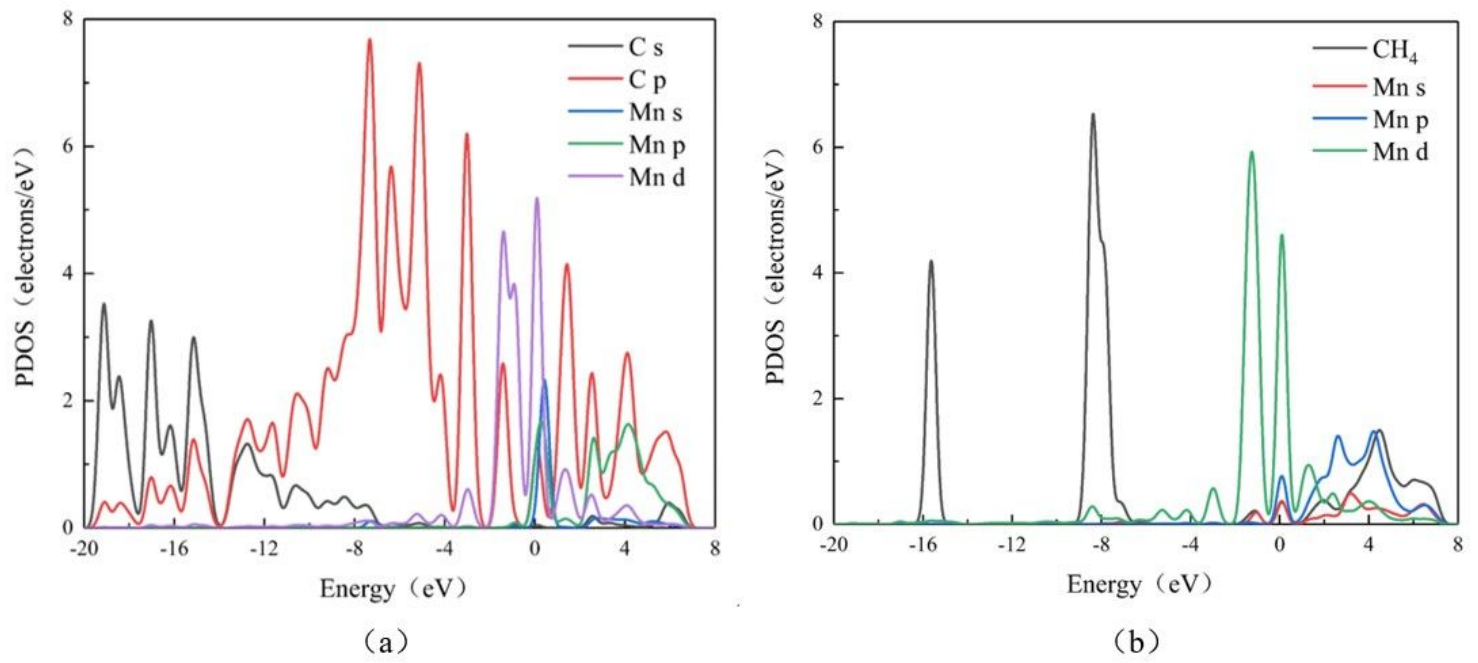


Figure 2

Geometric structure of the optimal adsorption position of a single CH<sub>4</sub> molecule on PG system.



**Figure 3**

PDOS of the system (a) Mn PG; (b) Mn PG adsorbs a CH<sub>4</sub>

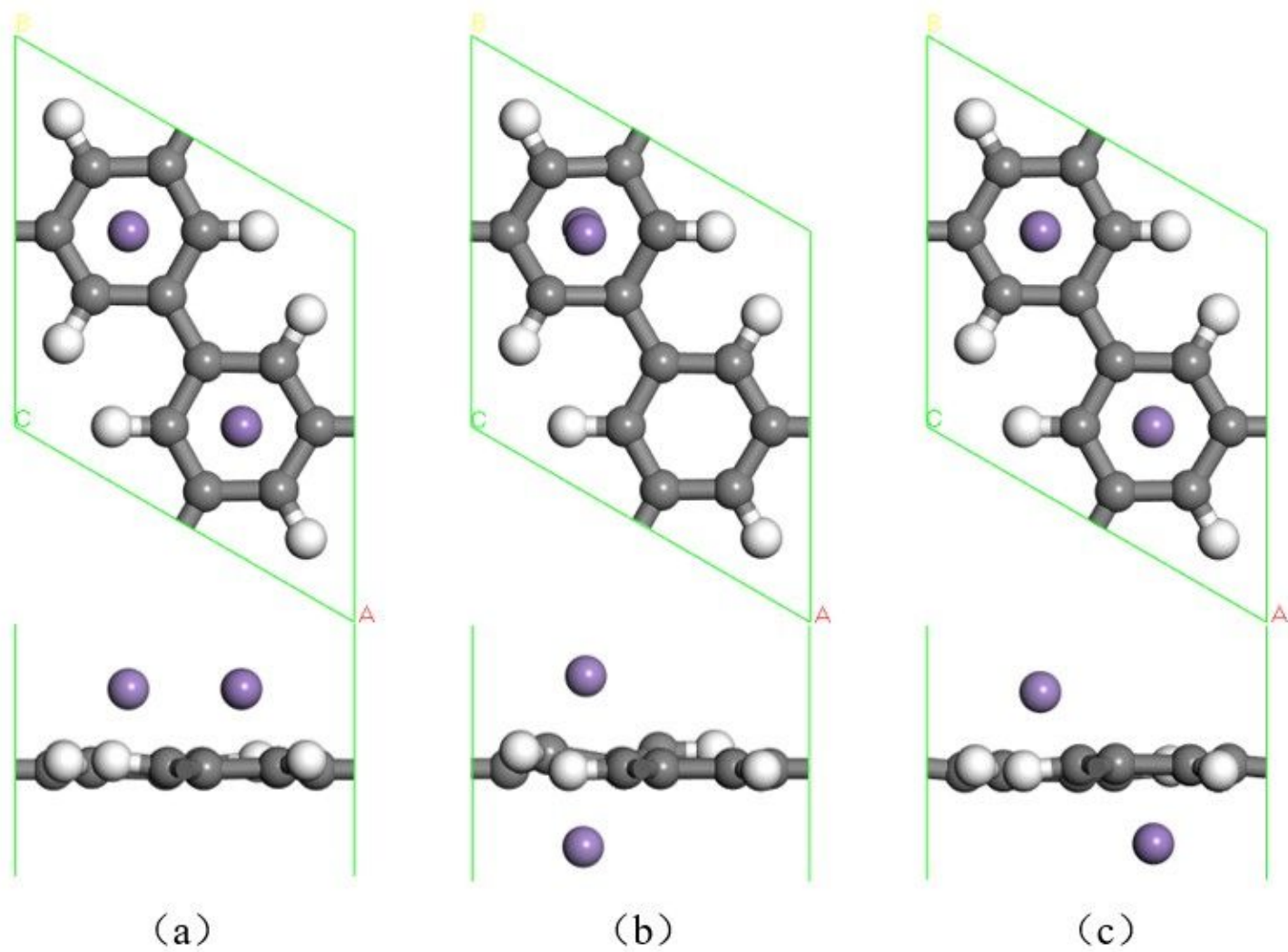


**Figure 4**

Three stable geometric structures of PG system modified by two Mn atoms.

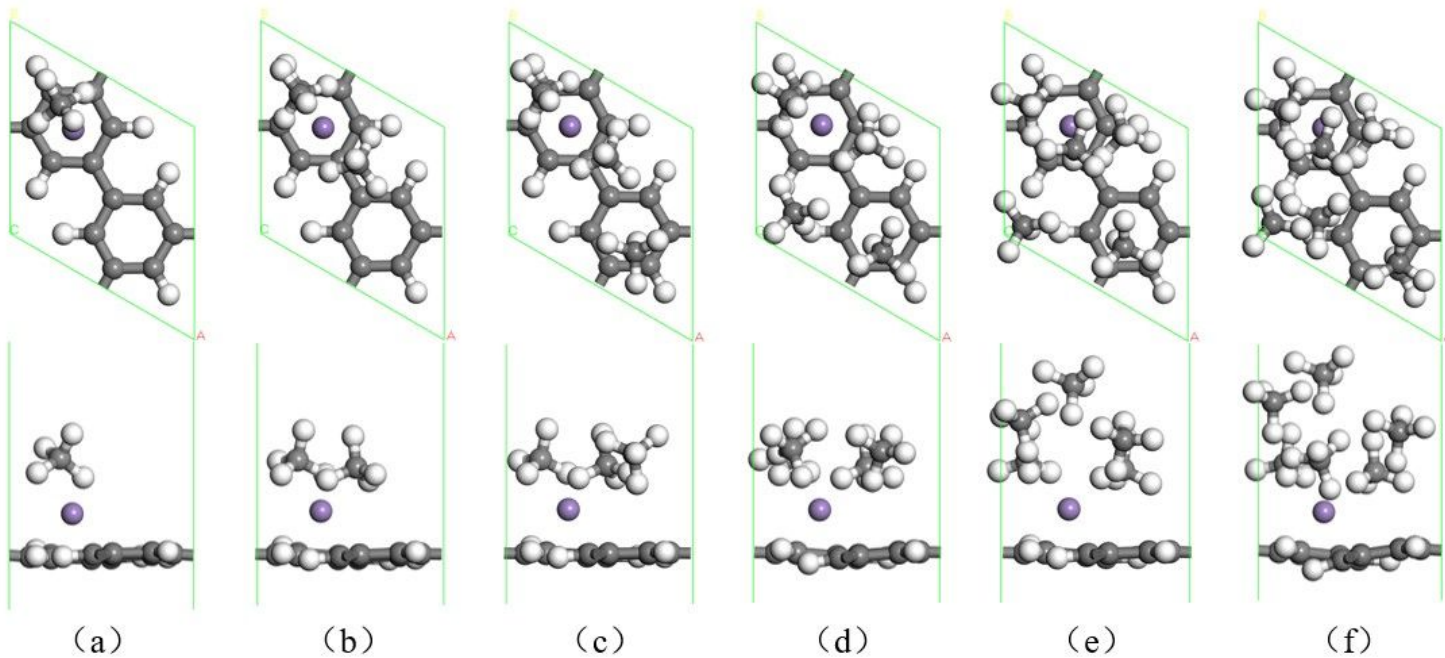


**Figure 5**

Geometric structure of Mn-PG system adsorbed 1-6 CH<sub>4</sub> molecules.

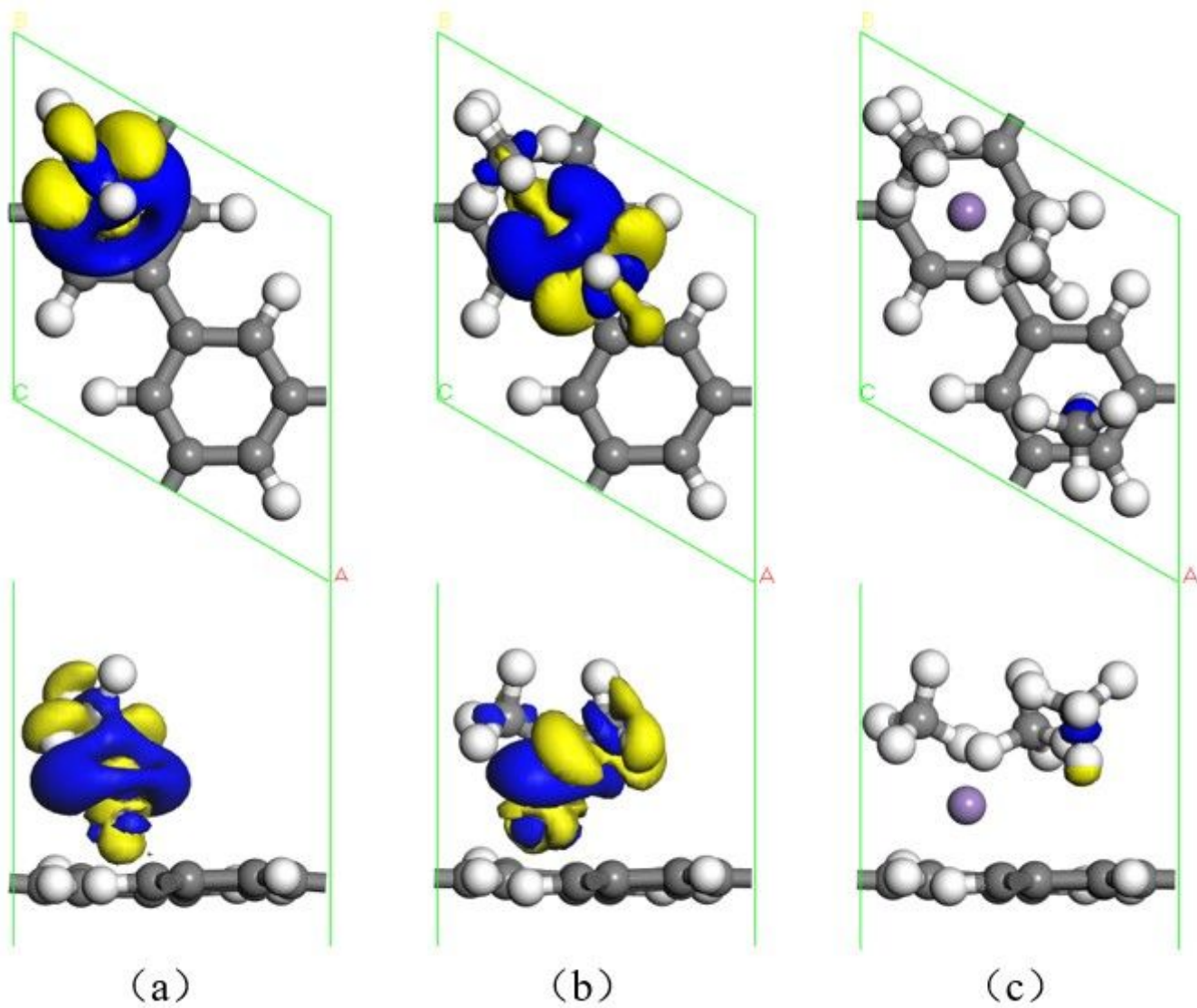
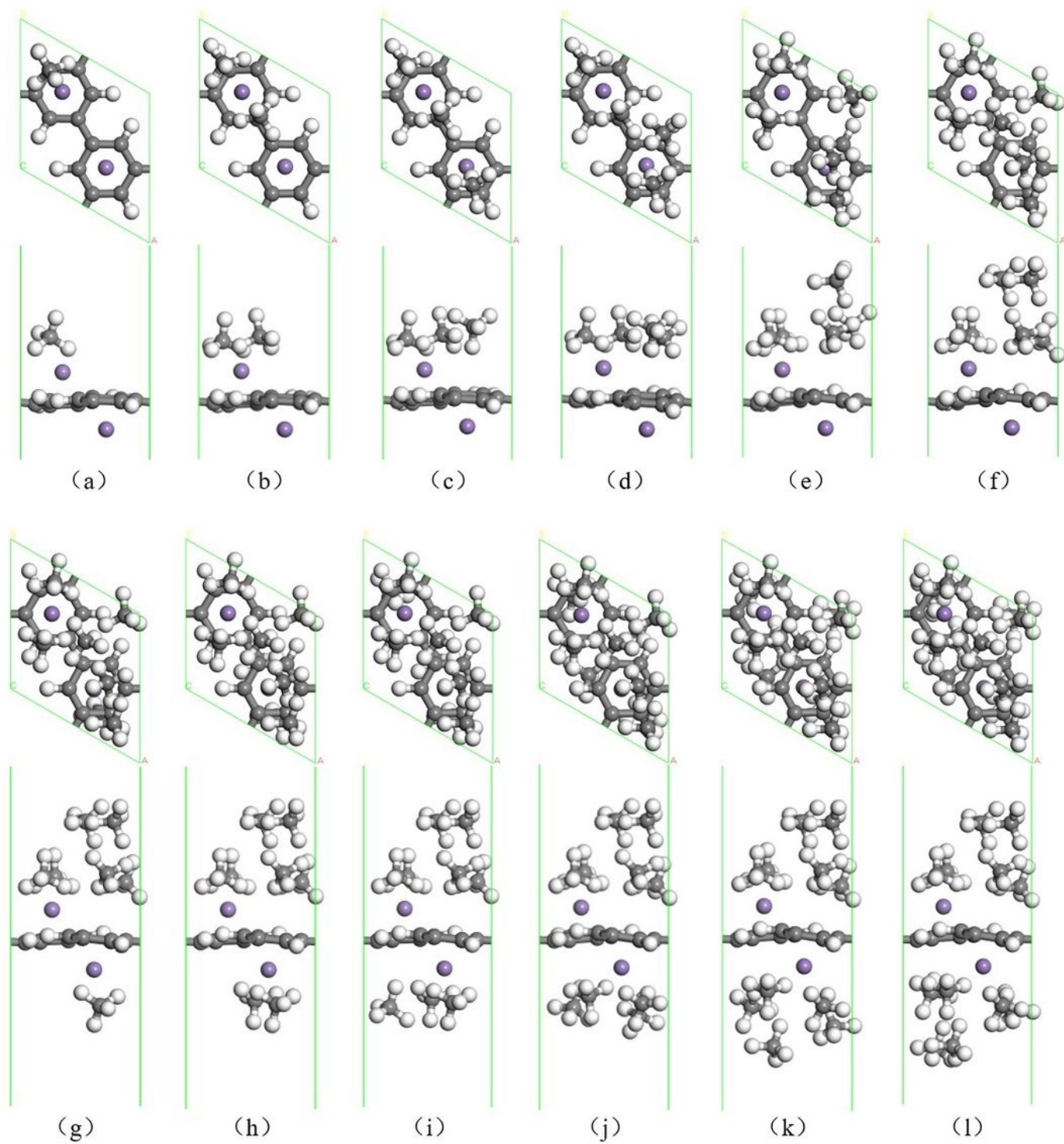


Figure 6

Charge difference density diagram of Mn-PG system adsorbed 1~3 CH<sub>4</sub> molecules.



**Figure 7**

Geometric structure of two Mn atoms modified PG system adsorbed 1~12 CH<sub>4</sub> molecules.

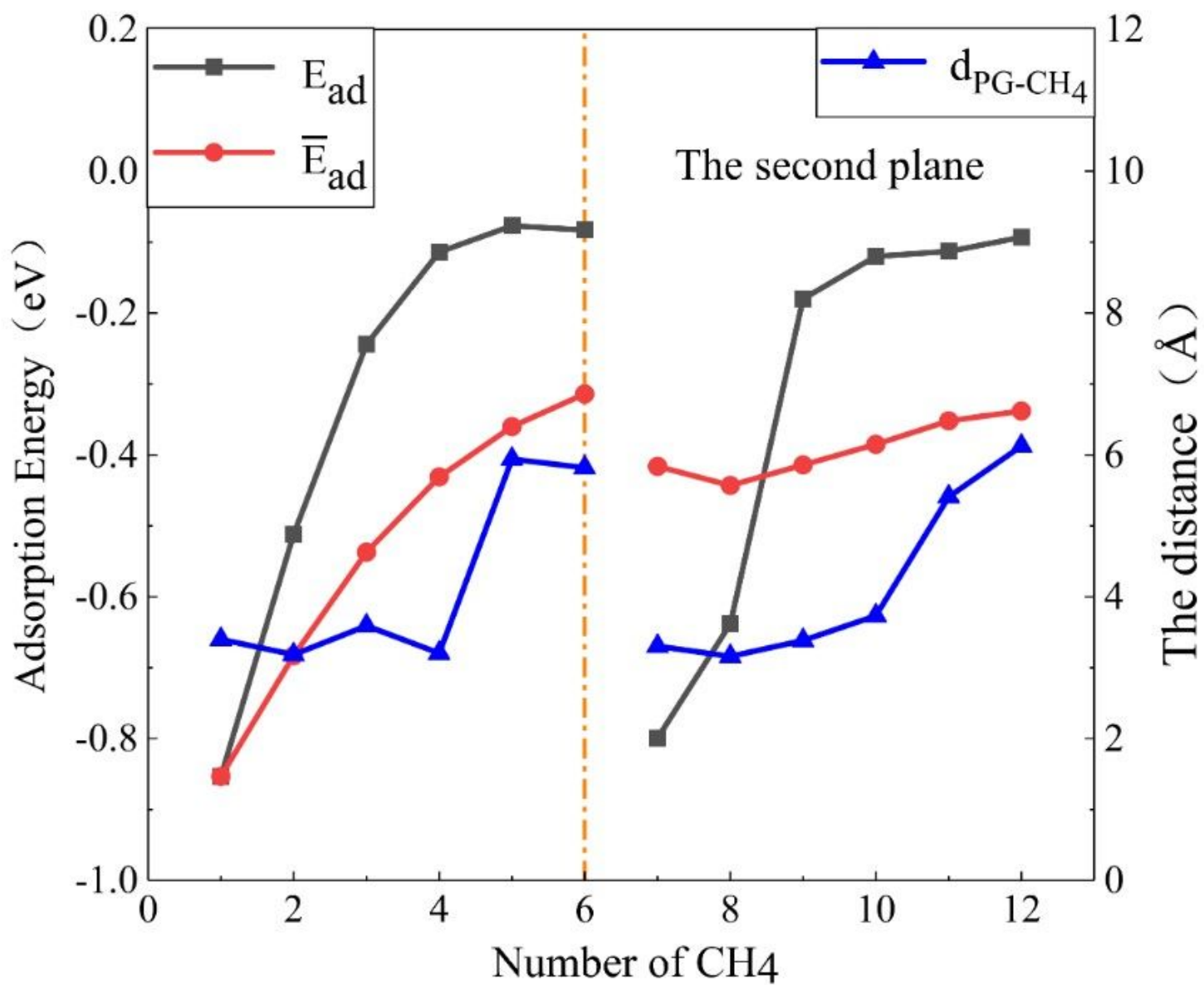
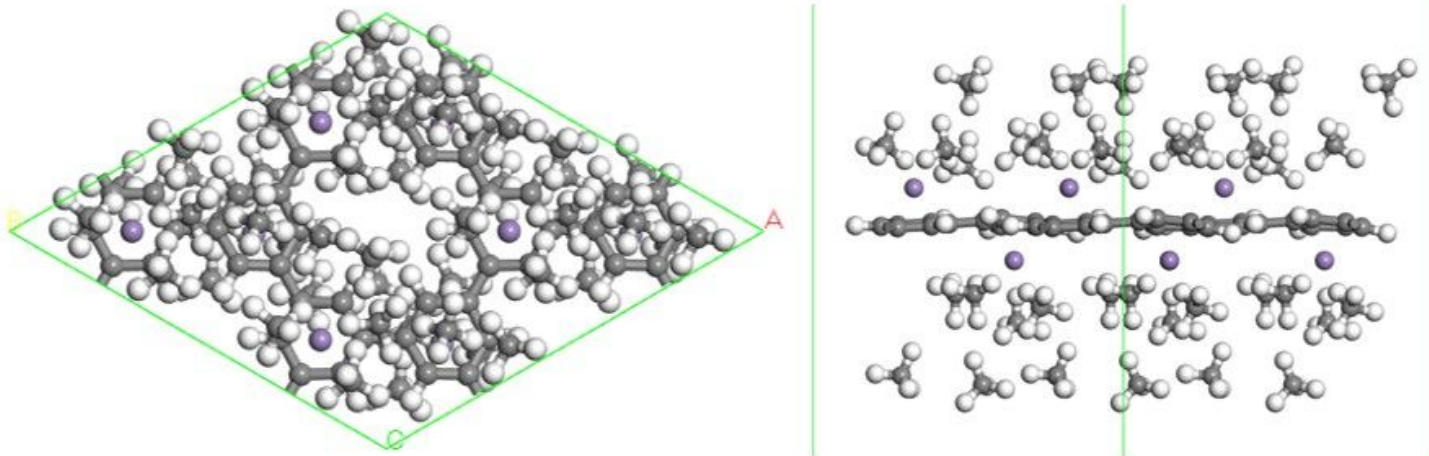


Figure 8

Energy parameters and geometric parameters of two Mn atoms modified PG system adsorbed 1~12 CH<sub>4</sub> molecules.



**Figure 9**

Geometric structure of Mn-PG supercell system adsorbed CH4 molecules.